

Elsevier Editorial System(tm) for Developmental Biology  
Manuscript Draft

Manuscript Number: DBIO-14-411R1

Title: Semi-Solid Tumor model in *Xenopus laevis*/gilli cloned tadpoles for Intravital study of neovascularization, immune cells and melanophore infiltration

Article Type: SI:*Xenopus* Disease models

Section/Category: Developmental Biology - Main

Keywords: Tumor model; angiogenesis; tumor immunity; intravital microscopy; tumor microenvironment

Corresponding Author: Dr. Jacques Robert,

Corresponding Author's Institution: University of Rochester

First Author: Nikesha Haynes-Gimore , PhD

Order of Authors: Nikesha Haynes-Gimore , PhD; Maureen Banach, BS; Edward B Brown, PhD; Ryan Dawes, BS; Eva-Stina Edholm, PhD; Minsoo Kim, PhD; Jacques Robert, PhD

Abstract: Tumors have the ability to grow as a self-sustaining entity within the body. This autonomy is in part accomplished by the tumor cells ability to induce the formation of new blood vessels (angiogenesis) and by controlling cell trafficking inside the tumor mass. These abilities greatly reduce the efficacy of many cancer therapies and pose challenges for the development of more effective cancer treatments. Hence, there is a need for animal models suitable for direct microscopy observation of blood vessel formation and cell trafficking, especially during early stages of tumor establishment. Here, we have developed a reliable and cost effective tumor model system in tadpoles of the amphibian *Xenopus laevis*. Tadpoles are ideally suited for direct microscopy observation because of their small size and transparency. Using the thymic lymphoid tumor line 15/0 derived from, and transplantable into, the *X. laevis*/gilli isogenic clone LG-15, we have adapted a system that consists in transplanting 15/0 tumor cells embedded into rat collagen under the dorsal skin of LG-15 tadpole recipients. This system recapitulates many facets of mammalian tumorigenesis and permits real time visualization of the active formation of the tumor microenvironment induced by 15/0 tumor cells including neovascularization, collagen rearrangements as well as infiltration of immune cells and melanophores.

DEPARTMENT OF MICROBIOLOGY & IMMUNOLOGY

Jacques ROBERT Ph. D.  
Associate Professor of Microbiology & Immunology  
601 Elmwood Avenue, Box 672  
Rochester, New York 14642  
Phone: (585) 275-1722  
FAX: (585) 473-9573  
E-mail [jacques\\_robert@urmc.rochester.edu](mailto:jacques_robert@urmc.rochester.edu)  
<http://www.urmc.rochester.edu/smd/mbi/faculty/robert.htm>  
<http://www.urmc.rochester.edu/smd/mbi/xenopus/index.htm>



UNIVERSITY of  
**ROCHESTER**  
MEDICAL CENTER

MEDICINE of THE HIGHEST ORDER

October 29, 2014

Dear Editor:

Enclosed, please find our revised manuscript entitled: “Semi-Solid Tumor model in *Xenopus laevis/gilli* cloned tadpoles for intravital study of neovascularization, immune cells and melanophore infiltration” that we would like to submit for consideration in The *Xenopus* Special Issue of *Developmental Biology* focusing on the strengths of this system for modeling human diseases and congenital defects, as well as for drug discovery.

We think that we have adequately addressed all the reviewer comments. We would like to thank the reviewers for their helpful comments and suggestions.

Thank you for your consideration.

Sincerely,

A handwritten signature in black ink, appearing to be 'J. Robert', written over a horizontal line.

Jacques Robert, Ph. D.  
Associate Professor of Microbiology and Immunology

RESPONSE TO REVIEWER'S COMMENTS:

Enclosed, please find a revision of our manuscript entitled: "Semi-Solid Tumor model in *Xenopus laevis/gilli* cloned tadpoles for Intravital study of neovascularization, immune cells and melanophore infiltration." We would like to thank the reviewers for their helpful comments and suggestions.

**Reviewer #1:**

This manuscript describes a new and novel in vivo model for observing tumor progression in vivo using an established *Xenopus* tumor cell line and syngeneic individual larvae. By culturing the tumor cells in collagen prior to implantation, the authors demonstrate the ability of these tumor cells to implant and expand and induce angiogenesis. As the authors suggest in their Discussion, this will provide a new model tumor progression, immune response to tumor engraftment and provide an in vivo system for screening compounds that regulate tumor progression and angiogenesis. It is appropriate for the Special Issue on *Xenopus* Disease Models.

Minor comments:

1. I would reword the first sentence of the second paragraph of the Introduction that states "Xenopus has been and still is the model system of choice for the study of fundamental questions related to development, immunology, toxicology, neurobiology, embryology and regenerative biology". Many readers who work with mouse, zebrafish, *Drosophila*, sea urchin etc may take offense at this claim. Perhaps a phrase such as: "Xenopus has been and still is one of the top model systems for the study of..."
2. Page 6, Methods - Preparation of tumor embedded collagen grafts. It would be helpful to define WT (presumably wild type).
3. Page 6, Methods - Preparation of tumor embedded collagen grafts. The authors describe experiments using shXNC10-deficient tumor cells, but I could not find these cells mentioned again in the results or discussion and saw no data using these cells.
4. Page 8, line 11. "water immersion" is repeated
5. Page 8, line 12. Please make the following match: "scattered/emitted light" and "emitted/scattered light"  
- Answer: Changes were made as suggested for points 1 to 5.

6. Figure 1 has arrows pointing to the growing tumor. If I understand the location of the tumors correctly, as the tumor changes at later stages the increase in melanocytes is obvious (specifically at day 24 and day 30, the tumors are black rather than white). This was a bit confusing as the increase in melanocytes is not discussed until later in the manuscript. It would be helpful if the authors provided a dashed line at the border to the tumor cells in panels AI - AVI. It would also be helpful if, in the figure legend, the authors mention the increase in melanocytes so the reader understands the change in color of the tumor.

- Answer: We added a dashed line to delineate the tumor graft and mentioned the accumulation of melanophores in the legend of figure 1.

7. Supplemental fig S4 is described in the text before Supplemental fig S3.  
- Answer: We changed the order of the Supplemental figs.

8. In the titles of multiple figure legends, the authors refer to "WT" tumor cells. Please spell out wild-type. Alternatively, if no experiments are presented that involve shXNC10-deficient tumor cells, is there a need to include "WT" in these legends?

- Answer: We have deleted WT in figure legends and in the text.

9. There is no legend for Figure 4!!!

- Answer: We apologize for this omission. We added a legend for figure 4

### **Reviewer #2:**

This manuscript presents results from a series of experiments characterizing a method for growth of tumors semi-solid medium in the *Xenopus* tadpole. The cells used to seed the tumors are immunologically matched to the particular *Xenopus* strain (*laevis/gilli* - LG) that acts as the host and therefore evade much of the immune response (I believe this is correct). Further studies follow the time course of tumor development and show that blood vessels growing into the tumors can be visualized in live embryos.

Overall, the manuscript is well written, the results are clearly presented and the data are convincing. The primary problem is that this is a fairly insubstantial piece of work and it does not address a specific biological question. The most focused contribution is the demonstration that growth and structure of blood vessels can be visualized in the live animal but the characterization is quite limited. As far as the studies go, the data are of good quality and the results are convincing.

Major points:

1. It is stated (p12) that blood flows through the tumor "at a slower rate than within normal tissue", but these data are not shown. The point is mentioned again in the discussion. I strongly suggest that the results be added to the manuscript.

- Answer: These are only observations not measurements. We have modified the text in the result section as follows:

“Although no specific measurement was performed, we observed that the rate of blood flow appeared to decrease upon entering the semi-solid tumor. In addition, some of the vasculature seemed to be either occluded and having turbulent blood flow, whereas other tumor vessels had slow laminar blood flow.”

We have also changed the discussion:

“The blood flow within 15/0 tumor vessels also appeared to be slower than in other adjacent healthy tissues as it is observed in mammalian tumors.”

2. Given that one of the primary claims of the work is that blood vessels can be imaged in live animals, the images shown in Fig. 3CIII and CIV, are fairly poor. It would also appear that these are relatively large vessels (e.g. compared to the scale of vessels shown in Fig. 3BI-III). The results would be more convincing if higher quality images could be provided.

- Answer: We have provided images of better quality (TIFF 300 dpi)

3. The relevance of the melanophore infiltration is difficult to understand (Fig. 4). Does this have a precedent in any known human tumor? What does it imply mechanistically? This observation is not clearly related to anything else in the paper and it would help if the presentation of the results could be more fully justified.

- Answer: We have added more rational and developed this section. At the beginning of the section page 14, we have added the following:

“In mammals, melanocytes are usually located within the basement membrane of the epidermis. The genetic alteration of essential signaling pathways within melanocytes often leads to malignant transformation, thus promoting the abnormal migration and accumulation of melanocytes resulting in melanoma [reviewed in (Uong and Zon, 2010)]. Therefore, the unusual tadpole melanophores infiltration into 15/0 tumor grafts warranted further examination. Increased infiltration of melanophores was observed in virtually all 15/0 tumor grafts from one week post-transplantation onward. Accumulation of these cells became more pronounced at later time points and at 3 weeks post-transplantation about 60% of the 15/0 graft were massively invaded and black in color as depicted in Fig 1A and 4A). »

Then: Penetration of melanophores inside the tumor mass is also evident in tissue sections of Figure 2B (especially panel VIII). To further characterize these melanophores and determine their proliferation capacity we tried to culture them *in vitro*.

At the of the section we added:

“In addition, since these cells are derived from LG-15 or LG-6 isogenic clones, adoptive cells transfer will be possible to determine their migration capability. “

In the discussion we added page 17:

“Such disorganization and abnormal accumulation of melanophores is reminiscent of melanoma lesions that often lead to skin cancer in human (Govindarajan et al., 2003; Uong and Zon, 2010). Whether tumor at advanced stage produce factors or induce inflammatory signals triggering the recruitment of these melanophores is currently unknown, but merit further investigation. This abnormal accumulation may correspond to the initial stage of malignant transformation that leads to melanoma in humans. *Xenopus* melanophores share many similarities with human melanocytes including their neural crest origin during embryogenesis (Le Douarin and Dupin, 2012). Importantly, neoplastic behavior of *Xenopus* melanophores can be induced (Blackiston et al., 2011; Mondia et al., 2011; Tomlinson et al., 2009). The ease to culture melanophores from 15/0 tumor grafts may afford a convenient source for further experimentation; in addition to the *Xenopus* melanophore cell lines that have been described (Carrithers et al., 1999; Iuga et al., 2009). An attractive feature of the present system is that the melanophore lines are derived from MHC-defined LG-6 or LG-15 isogenic clones and, therefore, can be adoptively transferred into LG-6 or LG-15 tadpole recipients for studying their neoplastic potential *in vivo*.”

Minor points:

1. The labeling Fig. 1B is unclear. Does "wild type" refer to 15/0 cells. Wouldn't a better control be non-tumor cells in collagen? In any case, the graph should be relabeled for clarity.

- Answer: We have removed wild type

2. It would be very useful if an extra sentence was added to the introduction, stating in simple terms (for non-immunologists) the reason for using the 15/0 cell line and the LG strain.

- Answer: We added the following sentence: “As in mammals, the 15/0 tumors can only be transplanted and grow in MHC compatible LG-6 and LG-15 cloned recipients, whereas they are rejected when transplanted into MHC mismatched strains and clones as well as into outbred animals. »

3. Add a sentence to the final part of the discussion explaining that use of *Xenopus* for study of tumor development (particularly for intravital studies) has ethical advantages over the use of mammalian models and is also preferred by animal care committees (particularly in the European system).

- Answer: Thank you for this suggestion. We added the following sentence: “It is also noteworthy that the use of cold blooded vertebrates such as *Xenopus* for study of tumor development (particularly for intravital studies) has ethical advantages over the use of mammalian models and is also preferred by animal care committees (particularly in the European system).”

4. The reference for Haynes-Gilmore in Carcinogenesis is missing.

- Answer: The reference has been updated

5. There are a number of minor typos, particularly in the Discussion.

6. Maybe reword sentence on top of p17. "convenient source for further experimentation; in addition to the *Xenopus* melanophore cell lines that have been described".

- Answer: Changed as suggested

## Highlights

- Development of a comparative intravital tumor model system in *Xenopus* tadpoles
- The system recapitulates many facets of mammalian tumorigenesis
- The active formation of the tumor microenvironment is visualized in real time
- Neoangiogenesis, and infiltration of immune cells and melanophores were visualized

**Semi-Solid Tumor model in *Xenopus laevis/gilli* cloned tadpoles for Intravital study of neovascularization, immune cells and melanophore infiltration**

Nikeshya Haynes-Gimore<sup>1,2</sup>, Maureen Banach<sup>1</sup>, Edward Brown<sup>3</sup>, Ryan Dawes<sup>3</sup>, Eva-Stina Edholm<sup>1</sup>, Minsoo Kim<sup>1,4</sup>, Jacques Robert<sup>1</sup>

<sup>1</sup> Department of Microbiology and Immunology, University of Rochester Medical Center, Rochester, USA

<sup>2</sup> Department of Pathology, University of Rochester Medical Center, Rochester, USA

<sup>3</sup> Department of Neurobiology and Anatomy, University of Rochester Medical Center, Rochester, USA

<sup>4</sup>Vaccine Center

Running Title: *Xenopus* tumor model

Keywords: Tumor model, angiogenesis, tumor immunity, intravital microscopy, tumor microenvironment

Communicating Author: Dr. Jacques Robert, Department of Microbiology and Immunology, University of Rochester Medical Center, Rochester, NY 14642; Phone (585) 275-1722; FAX (585) 473-9573; e-mail: [Jacques\\_Robert@urmc.rochester.edu](mailto:Jacques_Robert@urmc.rochester.edu)



**Abstract:**

Tumors have the ability to grow as a self-sustaining entity within the body. This autonomy is in part accomplished by the tumor cells ability to induce the formation of new blood vessels (angiogenesis) and by controlling cell trafficking inside the tumor mass. These abilities greatly reduce the efficacy of many cancer therapies and pose challenges for the development of more effective cancer treatments. Hence, there is a need for animal models suitable for direct microscopy observation of blood vessel formation and cell trafficking, especially during early stages of tumor establishment. Here, we have developed a reliable and cost effective tumor model system in tadpoles of the amphibian *Xenopus laevis*. Tadpoles are ideally suited for direct microscopy observation because of their small size and transparency. Using the thymic lymphoid tumor line 15/0 derived from, and transplantable into, the *X. laevis/gilli* isogenic clone LG-15, we have adapted a system that consists in transplanting 15/0 tumor cells embedded into rat collagen under the dorsal skin of LG-15 tadpole recipients. This system recapitulates many facets of mammalian tumorigenesis and permits real time visualization of the active formation of the tumor microenvironment induced by 15/0 tumor cells including neovascularization, collagen rearrangements as well as infiltration of immune cells and melanophores.

## **Introduction:**

Tumors have the remarkable ability to control the host microenvironment and promote blood vessel formation (angiogenesis) for enhancing their own growth, expansion and metastasis. Until recently, the formation of blood vessels was considered to be a process limited to embryogenesis. However, the formation of new blood vessels at later life stages is critical for tissue regeneration and wound healing processes [reviewed in (Tonnesen et al., 2000)]. Furthermore, angiogenesis is critical for tumorigenesis and metastasis as growing tumors require increasing amounts of oxygen and nutrients (Hanahan and Folkman, 1996). Once a growing tumor lesion exceeds a few millimeters, it initiates the development of new blood vessels from pre-existing host capillaries that are stimulated by pro-angiogenic signals expressed by tumor cells (Onimaru and Yonemitsu, 2011). Unlike normal tissues, the vasculature within the tumor mass is typically disorganized, leaky and the walls of tumor vessels are composed of both endothelial cells and tumor cells, which transform into “endothelial-like cells” (Chang et al., 2000; Maniotis et al., 1999). As such, there is a great fundamental and biomedical interest in understanding the dynamics of blood vessel formation during tumorigenesis, especially at the early stage of tumor establishment. To study this process *in vivo*, real time observation by intravital microscopy has gained much attention. To date this approach has been mainly developed in mouse and zebrafish models (Li et al., 2012; Nguyen et al., 2012; Painter and Ceol, 2014). However, the *Xenopus laevis* tadpoles could provide a useful alternative.

*Xenopus* has been and still is one of the top model systems for the study of fundamental questions related to development, immunology, toxicology, neurobiology, embryology and regenerative biology (Du Pasquier et al., 1989; Khokha, 2012; Robert and Ohta, 2009). More

recently *Xenopus* has also been increasingly used as a model for understanding tumor biology, transplantation biology, self tolerance and autoimmunity [reviewed in (Edholm and Robert, 2013)]. *Xenopus* possesses many attributes that make it an ideal model to study fundamental questions about tumor immunity and tumorigenesis including an external development, without maternal influences, thus providing convenient experimental manipulation at all stages of development. Elements that make the *Xenopus* tadpoles in particular attractive for experimentation are their transparency, small size (10-20 mm length) and as ectothermic vertebrates they tolerate room temperature and do not require highly aseptic conditions for observation, thus making them ideally suited for techniques such as intravital microscopy. Additionally, MHC-defined *X. laevis*/*X. gilli* (LG) isogenetic clones permit adoptive cell transfers (Kobel and Du Pasquier, 1975, 1977).

Importantly, *X. laevis* is the only known amphibian species with spontaneously arising and transplantable lymphoid tumors (Goyos and Robert, 2009). The 15/0 tumor cell line was derived from a spontaneous thymic tumor in the LG-15 clone (Robert et al., 1994). The *X. laevis* 15/0 tumor is highly tumorigenic and grows aggressively in both LG-15 and LG-6 adults and tadpoles, which share the same MHC haplotypes (a/c) but differ at multiple minor H loci. As in mammals, the 15/0 tumors can only be transplanted and grow in MHC compatible LG-6 and LG-15 cloned recipients, whereas they are rejected when transplanted into MHC mismatched strains and clones as well as into outbred animals. The 15/0 tumor can be easily distinguished from other cells by the surface expression of the immature thymocyte marker CTX (Du Pasquier and Robert, 1992; Robert and Cohen, 1998; Robert et al., 1994).

We have recently adapted for *Xenopus* a semi-solid tumor transplantation model to investigate the role of a nonclassical MHC molecule in tumor immune evasion (Haynes-Gilmore

et al., 2014). Tumor cells are transplanted into the LG-15 adult frogs subcutaneously, after which animals are monitored for date of first tumor appearance and tumor volume. The 15/0 tumors can then be palpated within 2 weeks of transplantation in healthy immunocompetent animals and within one month large solid tumors with metastatic outgrowths are typically observed in the spleen, liver and kidney (Robert et al., 1994). Conversely, 15/0 tumor cells are intraperitoneally transplanted into LG-15 tadpoles where it grows as an ascites within the peritoneum of larval recipients with frequent metastatic sites observed (Robert et al., 1994). Because of the difficulty of tracing tumor cells injected in suspension in the peritoneum, it is unclear as to what happens during the early stages of tumor establishment in *Xenopus* tadpole. In particular, the interactions of tumor cells with host immune effectors, the stroma and blood circulation at different stages of tumor development are still poorly characterized. A better understanding of the modalities of these interactions would be achieved by controlling the tumor's location as well as the direct visualization of the tumor fate. Thus, using the 15/0 tumor in the LG-15 and LG-6 tadpole system we developed a semi-solid tumor assay.

We demonstrate here a method for the intravital study of neoangiogenesis and tumor-immune interactions in the *X. laevis* tadpole, which may be subsequently used for the investigation of tumor microenvironmental interactions, as well as facilitate the discovery and development of new cancer immunotherapeutic and anti-angiogenic therapies.

## **Materials and Methods**

### **Animals**

LG-6 and LG-15 *Xenopus* cloned tadpoles were obtained from our breeding colony (<http://www.urmc.rochester.edu/smd/mbi/xenopus/index.htm>). These two clones are MHC identical (a/c) but differ at multiple minor histocompatibility loci. Transplanted 15/0 tumor cells grow similarly into both LG clones (Robert et al., 1994). All experiments were done with either stage 54-55 (two week old; (Nieuwkoop and Faber, 1967)) tadpoles or young (one year old) adults. Animals were anesthetized by immersion in tricaine methanesulfonate (TMS; 0.1g/L). All animals were handled under strict laboratory and UCAR regulations (Approval number 100577/2003-151) minimizing discomfort at all times.

### **Preparation of tumor embedded collagen grafts**

Setting solution (10x EBSS+0.2M  $\text{NaHCO}_3$ +0.15M NaOH) was added drop-wise to rat-tail collagen (BD Biosciences) on ice until the pH of the collagen was neutralized as previously described. The 15/0 tumor cells were then mixed with the collagen solution at a concentration of 500,000 cells per 10 $\mu$ L graft. Collagen/tumor mix was then pipetted into individual wells of 6 well plates and incubated at 27°C for 30 min to allow collagen polymerization. Two milliliters of 15/0 media, previously described [21] was added to 15/0 collagen grafts. Plates containing the grafts were then incubated at 27°C in chambers containing a blood gas mix (5%  $\text{CO}_2$ , 21%  $\text{O}_2$ , 74% N) until use.

### **Tumor grafts**

Small subcutaneous incisions were made on anterior left or right region of tadpoles and the collagen tumor grafts were inserted subcutaneously within the incision. Digital Images were

taken using an SMZ1500 Nikon stereomicroscope equipped with a DS-Qi1 monochrome cooled digital camera (Nikon) and areas of tumor grafts were determined using ImageJ software (NIH).

## **Histology**

Seven days post grafting, collagen embedded tumor grafts were removed and processed for cryosection. Serial 8 $\mu$ M sections were taken and 5<sup>th</sup> section was stained with haematoxylin and eosin (H&E) or Gömöri trichrome to distinguish collagen. Tumor collagen grafts were allowed to grow for three weeks when ascites fluid was removed and placed onto slide by cytospin then stained with Giemsa as previously described (Morales et al., 2010). Slides were examined using an Axiovert 200 inverted microscope and Infinity 2 digital camera (objective: 40/0.6, Zeiss).

## **Imaging of Semi-Solid Tumor Vasculature**

### *Ex vivo Conventional Fluorescence Imaging*

Anesthetized LG-15 tadpoles were injected intracardiacally with 10 $\mu$ L of 70,000MW (25mg/mL) Texas-red dextran (Invitrogen) to label the blood vessels. Approximately 10 minutes later 15/0-collagen tumor grafts were mounted onto slides and blood vessels and tumor cells were visualized using the Olympus BX40 conventional fluorescence microscope (Olympus America Inc.), and images acquired using the Retga 1300 camera (QImaging). Two-color images (Texas-red-dextran/PKH) were combined and analyzed using Image J software (NIH). For Confocal Intravital imaging: LG-6 tadpoles were anesthetized by immersion in TMS. They were then intracardiacally injected with 10 $\mu$ L of 70 000MW (25mg/mL) Texas-red dextran (Invitrogen) to label the blood vessels approximately 10 minutes before imaging. Animals were stabilized for imaging in between a solidified 1% agarose matrix made inside an imaging plate.

Image acquisition was conducted on an epifluorescence microscope (TE2000-U microscope; Nikon) using 4-20x objectives coupled to a Cool SNAP HQ CCD (Roger Scientific).

### *Multiphoton intravital imaging*

Approximately 10 minutes prior to imaging, anesthetized tadpoles were injected intracardiacally with 10  $\mu\text{L}$  of  $2 \times 10^6$  MW (2.5 mg/mL) tetramethyl rhodamine-conjugated dextran (Invitrogen) to label blood vessels. Intravital fluorescence and collagen second harmonic generation (SHG) microscopy were simultaneously performed using a custom multiphoton laser scanning microscope featuring a modified Fluoview FV300 confocal scan head (Olympus Optical) connected to a BX61WI upright microscope (Chen et al., 2012; Majewska et al., 2000). Excitation light was provided by a Mai Tai Ti:Sapphire laser (Spectra-Physics), delivering 810 nm light in 100 femtosecond pulses at 80 MHz. Prior to entering the scan box, laser light was circularly polarized by a Berek compensator (Model 5540, New Focus), thereby preventing the selective imaging of parallel-oriented collagen fibers (Campagnola, Nature Protocols 2012). An Olympus UMPLFL20XW water immersion objective (20x, 0.95 NA) was used to focus excitation light and collect emitted/scattered light. Emitted/scattered light (immunofluorescence and SHG, respectively) were separated from the excitation light by a 670 nm short-pass dichroic mirror. Tetramethyl rhodamine-conjugated dextran fluorescence was collected using a 605/55 nm bandpass filter (Chroma), while CFSE fluorescence was collected using a 535/40 nm bandpass filter (Chroma). Collagen SHG images were collected using a 405/30 nm bandpass filter (Semrock). Simultaneous tetramethyl-rhodamine/SHG and CFSE/SHG imaging were performed using a 565 nm dichroic mirror (Chroma). Fluorescence emission and SHG scattering were detected using non-descanned photomultiplier tubes (HC125-02; Hamamatsu) in whole

field detection mode. Images were acquired using Olympus Fluoview software at 1024 x 1024 pixels using Kalman averaging. Z stacks were constructed using a 10  $\mu$ M step size beginning at top most area of the graft just below the skin (to avoid cutaneous melanophores) and extending to the bottom of the graft (demarcated by the loss of detectable collagen SHG). Three-color images (TMR-dextran/CFSE/SHG) were combined and analyzed using ImageJ software (NIH).

### **Statistical analysis**

All quantitative data were analyzed using either students TTEST or a one-way ANOVA using the Vassar Stat software ([www.vassarstats.net](http://www.vassarstats.net)).

### **Results:**

#### *Growth of the 15/0 tumor within semi-solid tumor grafts*

The thymic lymphoid 15/0 tumor grows robustly *in vivo* when transplanted intraperitoneally into genetically compatible LG-15 or LG-6 cloned tadpoles (Robert et al., 1994). However, this type of transplantation is not suitable for direct observation of tumor architecture and tumor-induced neovascularization. Owing to the transparency of the tadpoles' skin we reasoned that the immobilization of tumor cells on a solid matrix would permit such visualization. Thus, we embedded 15/0 tumor cells into rat-tail type I collagen. Once polymerized, the tumor was engrafted subcutaneously on the anterior left and right regions of two-week old LG-15 or LG-6 tadpoles (Figure S1).

For the initial assessment of this tumor assay, we delineated the *in vivo* growth potential of the 15/0 containing collagen (15/0-collagen) semi-solid grafts within syngeneic LG-15 tadpoles.



Animals were subcutaneously grafted with either collagen alone or 15/0-collagen, and then tumor growth was monitored over time (Figure 1A). The 15/0-collagen grafts showed steady growth over a one-month period, whereas collagen alone grafts showed little to no changes of the relative area compared to day 0 indicating that tadpoles tolerated the rat collagen (Figure 1B). We next determined whether the 15/0 tumor cells could be visualized within the 15/0-collagen grafts. Accordingly, we performed intra-vital multiphoton imaging on LG-6 tadpoles grafted with CFSE-labeled 15/0 tumor collagen embedded grafts. After one week of *in vivo* growth, numerous CFSE fluorescent 15/0 tumor cells were detected within the collagen matrix (Figure S2 and 3C), indicating that the 15/0 tumor cells within the collagen grafts were proliferating.

#### *Visualization of tumor cells within the collagen matrix of the semi-solid graft*

We next determined the ability of rat collagen to allow *Xenopus* 15/0 tumor cell growth *in vitro* and *in vivo*. 15/0 tumor cells were embedded into collagen and maintained either in *in vitro* culture for 9 days (tissue culture conditions described in the methods) or subcutaneously grafted into LG-15 tadpoles for 9 days after which the grafts were removed and cells were visualized using the nuclear DAPI counter staining. Both in *in vitro* (Figure 2A, I and IV) and *in vivo* (Figure 2A; II and V) conditions, 15/0 cells accumulated throughout the graft and no marked apoptosis (e.g., picnotic nuclei) was noted. Combined, these results show that the embedding of the 15/0 tumor cells within the collagen does not hinder the proliferation and viability of the tumor cells.

To further characterize the *in vivo* growth of the collagen-embedded 15/0 tumor grafts, we performed histological analysis on cryosection of tumor-bearing animals at varying times post-implantation. H&E staining of cryosections containing tumor graft as well as the eye and portion

of the brain were obtained. Interestingly, as the tumor progressed and increased in volume, there were considerable morphological and positional changes of the tumor cells within the collagen matrix. During the first few days after tumor engraftment, tumor cells were irregularly interspaced throughout the graft with no discernible patterns (Figure 2B, I and V). Tumor cells exhibited a rounded morphology. As tumorigenesis progressed, significant tumor morphogenesis was observed (Figure 2B, II-II and VI-VII) with “granuloma like” structures observed at day 30 (Figure 2B, IV and VIII). The tumor cells took on a stretched out, stromal morphology, forming swirl like structures.

To reveal possible modification of the collagen matrix during tumor progression we stained the tissues with Gömöri trichrome, which distinguishes plasma from connective tissue including collagen. At early time points following of tumor engraftment (Day 3), 15/0-collagen grafts exhibited diffuse spatial patterning of collagen, with pockets of tumor cells throughout the graft including some areas of collagen void of tumor cells (Figure 2C, I and V). At intermediate time points (days 10-16) post-tumor engraftment, more organized collagen fibrils were detected within the graft and tumor cells were more uniformly dispersed throughout the tumor mass, typically lining up along the collagen fibers (Figure 2B II-III, VI-VII). In the more advanced stage of tumor growth (30 days post- engraftment), tumor cells along with invading melanophores and immune cells were organized in a stratified layer pattern surrounding the remaining collagen forming “granuloma-like” structures (Figure 2B IV and VII)

Collectively, these data show not only that the 15/0 tumor cells are able to effectively grow within rat collagen embedded grafts but also that these tumor cells undergo morphogenetic changes resulting in the reorganization of the tumor microenvironment.

### *Visualization of neo-angiogenesis within the semi solid tumor graft*

Solid tumors usually require additional nutrients to support growth once its dimensions surpass a few millimeters. Given the steady growth of 15/0 tumor within the grafted collagen mass, we reasoned that initiation of neovasculature should occur to support continuous growth. To assess the formation of new vasculature inside 15/0 tumor-collagen grafts, we grafted collagen embedded with 15/0 tumor cells labeled with the plasma membrane fluorescent dye PKH-26. At different time points post-grafting, anesthetized animals were intracardiacally infused with Texas-red labeled dextran and given time (10 minutes) to allow for complete circulation of the dye throughout the tadpole vasculature before removing the grafts for imaging. Texas-red dextran filled vasculature was observed in 15/0-collagen grafts within seven days following engraftment (Figure 3A and S4). These vessels displayed varying sizes (2 to 10  $\mu\text{m}$  diameter), shapes and branching patterns within the collagen tumor.

To further visualize the tumor neovasculature, we performed intra-vital imaging of Texas-red loaded vessels within 15/0-collagen grafts in tadpole recipients 2 weeks post-implantation. Bright field observation showed blood flow within the tumor and surrounding tissue (Figure 3B; I). Although no specific measurement was performed, we observed that the rate of blood flow appeared to decrease upon entering the semi-solid tumor. In addition, some of the vasculature seemed to be either occluded and have turbulent blood flow, whereas other tumor vessels had slow laminar blood flow. To further confirm the presence of vasculature within the tumor and whether the normal vasculature branched into the tumor vasculature, we examined the Texas-red fluorescence in and around the tumor. As depicted in Figure 3B, Texas-red fluorescence revealed larger vessels entering the tumor that branched into multiple smaller vessels gradually

progressing deeper into the tumor (Figure 3B). Imaging further into the tumor revealed a convoluted network of blood vessels (Figure 3C).

To further elucidate the complexity of the tumor microenvironment, we adapted a two photon imaging system such that we could simultaneously monitor tumor cells, tumor vasculature and immune effector cells within the collagen matrix. Taking advantage of the inherent physical and structural properties of type I collagen, we imaged the collagen matrix using multiphoton SHG microscopy. We initially tested whether we could detect vasculature and collagen intravitaly in our tadpole model system. Indeed, Texas-red filled normal vasculature (Figure S3A) and SHG in non-tumor cells bearing collagen grafts (Figure S3B) could be visualized within LG-15 tadpoles. We then proceeded to observe tumor angiogenesis within LG-15 and LG-6 tadpole recipients grafted with 15/0-embedded collagens. Initial intravital imaging sessions demonstrated that the 70,000 MW TRITC dextran used in the above experiments rapidly leaked from vessels nearby tumors, thus necessitating the use of a higher molecular weight fluorescent dextran (tetra methyl rhodamine  $2 \times 10^6$  MW (TMR) dextran) to ensure confined labeling of tumor-associated vessels. Collagen grafts containing CFSE-labeled 15/0 tumor cells were implanted into both LG-15 and LG-6 tadpoles and intravital multiphoton imaging was performed at varying time points between 1 and 2 weeks. We observed TMR dextran filled vasculature in the tumor graft in both LG-15 and LG-6 hosts as evidenced by overlapping TMR staining with CFSE fluorescence cells and SHG collagen signal (Figure 3C). It is noteworthy that the SHG signal became undetectable in advanced 15/0-collagen grafts after approximately two weeks post-transplantation, but not in grafts of collagen alone at similar time points (data not shown), suggesting that the growing 15/0 tumor cells readily modified the transplant collagen matrix.

*Induced migration of melanophores into 15/0 semi-solid tumor grafts.*

During tumor engraftment experiments we noticed that 15/0 tumor-embedded collagen (Figure 4A) but not collagen only grafts (Figure 1A) became heavily infiltrated with melanophores. In mammals, melanocytes are usually located within the basement membrane of the epidermis. The genetic alteration of essential signaling pathways within melanocytes often leads to malignant transformation, thus promoting the abnormal migration and accumulation of melanocytes resulting in melanoma [reviewed in (Uong and Zon, 2010)]. Therefore, the unusual tadpole melanophores infiltration into 15/0 tumor grafts warranted further examination. Increased infiltration of melanophores was observed in virtually all 15/0 tumor grafts from one week post-transplantation onward. Accumulation of these cells became more pronounced at later time points and at 3 weeks post-transplantation about 60% of the 15/0 graft were massively invaded and black in color as depicted in Fig 1A and 4A). Within these larger more advanced tumor grafts, melanophores accumulated not only at the surface of the graft but also invaded deeply inside of the tumor mass (Figure 4B). *Ex vivo* bright field imaging of these 15/0-collagen grafts showed that melanophores migrated into the whole tumor graft spreading their dendrites throughout the collagen matrix and tumor cells (Figure 4C). Penetration of melanophores inside the tumor mass is also evident in tissue sections of Figure 2B (especially panel VIII) and Figure 3B. To further characterize these melanophores and determine their proliferation capacity we cultured them *in vitro*. To obtain enriched melanophores cultures we took advantage of the fact that 15/0 tumor cells are unable to survive when cultured in amphibian culture medium without normal *Xenopus* serum supplementation (Robert et al., 1994). This allowed us to obtain cell culture constituted mainly of melanophores and fibroblast surviving more than 4 weeks, albeit not proliferating *in vitro* (Figure 4D). Nevertheless the possibility to obtain relatively number large numbers (1-2 x

$10^6$  cells per tadpoles) of melanophores in culture should be of interest for further investigation. In addition, since these cells are derived from LG-15 or LG-6 isogenic clones, adoptive cells transfer will be possible to determine their migration capability.

## **Discussion.**

The semi-solid tumor engraftment system we have adapted in *Xenopus* tadpoles provides an attractive comparative system for gathering new insights into the development and establishment of the tumor microenvironment. The 15/0 thymic lymphoid tumor and the *Xenopus* host immune response are relatively well characterized (reviewed in (Goyos and Robert, 2009)). Here, we have established the initial conditions to visualize in real time the active formation of the tumor microenvironment induced by 15/0 tumor cells including neovascularization, collagen rearrangements as well as infiltration of melanophores.

How tumor cells modify their surrounding microenvironment i.e. immune mediators, stromal cells, extracellular matrix proteins as well as neo-angiogenesis is an active area of research owing to the fact that these interactions are crucial for promoting tumor growth and invasiveness (Weis and Cheresh, 2011). Tumor angiogenesis is essential to support and promote growth and metastasis. Thus, understanding blood vessel formation during tumorigenesis may provide new ways in which tumor vasculature can be manipulated for the treatment of cancer. For the first time in a frog model we have shown rapid robust tumor vessel neo-formation, which recapitulates many properties already described in human tumor angiogenesis. The neovascularization occurring in the 15/0 tumor engraftment in the *Xenopus* tadpole presents many similarities with mammalian tumor angiogenesis. In particular, similar to mammals, 15/0 tumor-induced angiogenesis results in the formation of a disorganized blood vessel network with

intricate branching and anastomosis (Yang et al., 2001). The blood flow within 15/0 tumor vessels also appeared to be slower than in other adjacent healthy tissues as it is observed in mammalian tumors. Notably, the vascular disorganization is thought to be one of the reasons that intravenous chemotherapies are not fully effective. This is due to the difficulty of efficiently perfusing the tumor with chemotherapeutic agents as a result of the disorganized properties of the tumor vasculature (Kerbel, 2000). The transparency of the tadpole skin and its tolerance to room temperature are convenient attributes for intravital observation of early stages of neovascularization that start within a few days after engraftment.

Also reminiscent of mammalian tumor establishment is the reorganization and degradation of the extracellular matrix here constituted mainly of type I rat collagen (Figure 2). Collagen is one of numerous components of the cellular microenvironment. How tumor cells are able to modify the collagen and whether this modification leads to any metastatic out growth is an active area of research. Interestingly, it is known that in many cancers the modification of the extracellular matrix is necessary for metastatic outgrowth [reviewed in (Lu et al., 2012)]. For example, type I collagen produced by stromal fibroblast in the tumor microenvironment can promote tumor growth in breast cancer (Kim et al., 2014). In addition, tumor cells are known to secrete enzymes such as metalloproteases to degrade extracellular matrix including collagen to facilitate invasion (Zhang et al., 2014). Thus, using our model we can now study how collagen modification can modulate tumor growth.

For effective and sustained growth, tumor cells have to elude host defense mechanisms ideally suited to effectively recognize and destroy cells undergoing neoplastic transformations

(Gajewski et al., 2011). Notably, tumors promote potent suppressive environment by recruiting a variety of suppressive leukocytes such as macrophages (Marigo et al., 2008; Shevach, 2009; Sica et al., 2008). Our study shows that we can effectively visualize tumor cells within the collagen matrix in living hosts (Figure 3C). Previously we have shown that though the modification of immune molecules present on tumor cells, we can enhance the infiltration of leukocytes into the collagen tumor graft (Haynes-Gilmore et al., 2014). Thus, it will be possible in future experiments to visualize in real time interactions between tumor and immune cells in conjunction with transgenic approach (Nedelkovska and Robert, 2012). Intriguingly, semi-solid 15/0 tumor grafts at later stages (about 2 weeks post-grafting) also became infiltrated by high numbers of melanophores. Such disorganization and abnormal accumulation of melanophores is reminiscent of melanoma lesions that often lead to skin cancer in human (Govindarajan et al., 2003; Uong and Zon, 2010). Whether tumor at advanced stage produce factors or induce inflammatory signals triggering the recruitment of these melanophores is currently unknown, but merit further investigation. This abnormal accumulation may correspond to the initial stage of malignant transformation that leads to melanoma in humans. *Xenopus* melanophores share many similarities with human melanocytes including their neural crest origin during embryogenesis (Le Douarin and Dupin, 2012). Importantly, neoplastic behavior of *Xenopus* melanophores can be induced (Blackiston et al., 2011; Mondia et al., 2011; Tomlinson et al., 2009). The ease to culture melanophores from 15/0 tumor grafts may afford a convenient source for further experimentation; in addition to the *Xenopus* melanophore cell lines that have been described (Carrithers et al., 1999; Iuga et al., 2009). An attractive feature of the present system is that the melanophore lines are derived from MHC-defined LG-6 or LG-15 isogenic clones and, therefore,



can be adoptively transferred into LG-6 or LG-15 tadpole recipients for studying their neoplastic potential *in vivo*.

As a final remark, it is noteworthy that the use of cold blooded vertebrates such as *Xenopus* for studying tumor development (particularly for intravital studies) has ethical advantages over the use of mammalian models and is also preferred by animal care committees.

In conclusion, we have developed a novel intra-vital semi-solid tumor model in transparent tadpoles, which recapitulates many of the functional characteristics of mammalian tumorigenesis. The availability of a reliable comparative model that is cost-effective and easily accessible to manipulation should reveal useful for the development of new drugs targeting angiogenesis and extracellular matrix or promoting antitumor immunity.

### **Acknowledgements**

We would like to thank Tina Martin for the expert animal husbandry and Dr. Leon Grayfer for discussions and critical reading of the manuscript. This research was supported by the National Institutes of Health Grant R24-AI-059830, a University of Rochester Wilmot Cancer Center Seed grant and support from the Kesel Fund of Rochester Area Community Foundation, Rochester NY.

### **Disclosures/Conflicts of Interest**

The authors disclose no conflicts of interest.

## References

- Blackiston, D., Adams, D.S., Lemire, J.M., Lobikin, M., Levin, M., 2011. Transmembrane potential of GlyCl-expressing instructor cells induces a neoplastic-like conversion of melanocytes via a serotonergic pathway. *Dis Model Mech* 4, 67-85.
- Carrithers, M.D., Marotti, L.A., Yoshimura, A., Lerner, M.R., 1999. A Melanophore-Based Screening Assay for Erythropoietin Receptors. *Journal of biomolecular screening* 4, 9-14.
- Chang, Y.S., di Tomaso, E., McDonald, D.M., Jones, R., Jain, R.K., Munn, L.L., 2000. Mosaic blood vessels in tumors: frequency of cancer cells in contact with flowing blood. *Proc Natl Acad Sci U S A* 97, 14608-14613.
- Chen, X., Nadiarynkh, O., Plotnikov, S., Campagnola, P.J., 2012. Second harmonic generation microscopy for quantitative analysis of collagen fibrillar structure. *Nature protocols* 7, 654-669.
- Du Pasquier, L., Robert, J., 1992. In vitro growth of thymic tumor cell lines from *Xenopus*. *Dev Immunol* 2, 295-307.
- Du Pasquier, L., Schwager, J., Flajnik, M.F., 1989. The immune system of *Xenopus*. *Annu Rev Immunol* 7, 251-275.
- Edholm, E.-S., Robert, J., 2013. Recent Research Progress and Potential Uses of the Amphibian *Xenopus* as a Biomedical and Immunological Model System. *Resources*.
- Gajewski, T.F., Fuertes, M., Spaapen, R., Zheng, Y., Kline, J., 2011. Molecular profiling to identify relevant immune resistance mechanisms in the tumor microenvironment. *Curr Opin Immunol* 23, 286-292.
- Govindarajan, B., Bai, X., Cohen, C., Zhong, H., Kilroy, S., Louis, G., Moses, M., Arbiser, J.L., 2003. Malignant transformation of melanocytes to melanoma by constitutive activation of mitogen-activated protein kinase kinase (MAPKK) signaling. *J Biol Chem* 278, 9790-9795.
- Goyos, A., Robert, J., 2009. Tumorigenesis and anti-tumor immune responses in *Xenopus*. *Front Biosci (Landmark Ed)* 14, 167-176.
- Hanahan, D., Folkman, J., 1996. Patterns and emerging mechanisms of the angiogenic switch during tumorigenesis. *Cell* 86, 353-364.
- Haynes-Gilmore, N., Banach, M., Edholm, E.S., Lord, E., Robert, J., 2014. A critical role of non-classical MHC in tumor immune evasion in the amphibian *Xenopus* model. *Carcinogenesis* 35, 1807-1813.
- Iuga, A., Lerner, E., Shedd, T.R., van der Schalie, W.H., 2009. Rapid responses of a melanophore cell line to chemical contaminants in water. *Journal of applied toxicology : JAT* 29, 346-349.
- Kerbek, R.S., 2000. Tumor angiogenesis: past, present and the near future. *Carcinogenesis* 21, 505-515.
- Khokha, M.K., 2012. *Xenopus* white papers and resources: folding functional genomics and genetics into the frog. *Genesis* 50, 133-142.
- Kim, S.H., Lee, H.Y., Jung, S.P., Kim, S., Lee, J.E., Nam, S.J., Bae, J.W., 2014. Role of secreted type I collagen derived from stromal cells in two breast cancer cell lines. *Oncology letters* 8, 507-512.
- Kobel, H.R., Du Pasquier, D., 1975. "Production of Large Clones of Histocompatible, Fully Identical Clawed Toads (*Xenopus*).". *Immunogenetics* 2, 87-91.
- Kobel, H.R., Du Pasquier, D., 1977. Strains and species of *Xenopus* for immunological research. *Developmental Immunobiology*.

Le Douarin, N.M., Dupin, E., 2012. The neural crest in vertebrate evolution. *Current opinion in genetics & development* 22, 381-389.

Li, L., Yan, B., Shi, Y.Q., Zhang, W.Q., Wen, Z.L., 2012. Live imaging reveals differing roles of macrophages and neutrophils during zebrafish tail fin regeneration. *J Biol Chem* 287, 25353-25360.

Lu, P., Weaver, V.M., Werb, Z., 2012. The extracellular matrix: a dynamic niche in cancer progression. *The Journal of cell biology* 196, 395-406.

Majewska, A., Yiu, G., Yuste, R., 2000. A custom-made two-photon microscope and deconvolution system. *Pflugers Archiv : European journal of physiology* 441, 398-408.

Maniotis, A.J., Folberg, R., Hess, A., Seftor, E.A., Gardner, L.M., Pe'er, J., Trent, J.M., Meltzer, P.S., Hendrix, M.J., 1999. Vascular channel formation by human melanoma cells in vivo and in vitro: vasculogenic mimicry. *Am J Pathol* 155, 739-752.

Marigo, I., Dolcetti, L., Serafini, P., Zanovello, P., Bronte, V., 2008. Tumor-induced tolerance and immune suppression by myeloid derived suppressor cells. *Immunol Rev* 222, 162-179.

Mondia, J.P., Adams, D.S., Orendorff, R.D., Levin, M., Omenetto, F.G., 2011. Patterned femtosecond-laser ablation of *Xenopus laevis* melanocytes for studies of cell migration, wound repair, and developmental processes. *Biomed Opt Express* 2, 2383-2391.

Morales, H.D., Abramowitz, L., Gertz, J., Sowa, J., Vogel, A., Robert, J., 2010. Innate immune responses and permissiveness to ranavirus infection of peritoneal leukocytes in the frog *Xenopus laevis*. *J Virol* 84, 4912-4922.

Nedelkovska, H., Robert, J., 2012. Optimized transgenesis in *Xenopus laevis/gilli* isogenetic clones for immunological studies. *Genesis* 50, 300-306.

Nguyen, A.T., Emelyanov, A., Koh, C.H., Spitsbergen, J.M., Parinov, S., Gong, Z., 2012. An inducible kras(V12) transgenic zebrafish model for liver tumorigenesis and chemical drug screening. *Disease models & mechanisms* 5, 63-72.

Nieuwkoop, P.D., Faber, J., 1967. Normal table of *Xenopus laevis* (Daudin) : a systematical and chronological survey of the development from the fertilized egg till the end of metamorphosis, Amsterdam : North-Holland.

Onimaru, M., Yonemitsu, Y., 2011. Angiogenic and lymphangiogenic cascades in the tumor microenvironment. *Front Biosci (Schol Ed)* 3, 216-225.

Painter, C.A., Ceol, C.J., 2014. Zebrafish as a platform to study tumor progression. *Methods in molecular biology (Clifton, N.J.)* 1176, 143-155.

Robert, J., Cohen, N., 1998. Ontogeny of CTX expression in xenopus. *Dev Comp Immunol* 22, 605-612.

Robert, J., Guet, C., Du Pasquier, L., 1994. Lymphoid tumors of *Xenopus laevis* with different capacities for growth in larvae and adults. *Dev Immunol* 3, 297-307.

Robert, J., Ohta, Y., 2009. Comparative and developmental study of the immune system in *Xenopus*. *Dev Dyn* 238, 1249-1270.

Shevach, E.M., 2009. Mechanisms of foxp3+ T regulatory cell-mediated suppression. *Immunity* 30, 636-645.

Sica, A., Larghi, P., Mancino, A., Rubino, L., Porta, C., Totaro, M.G., Rimoldi, M., Biswas, S.K., Allavena, P., Mantovani, A., 2008. Macrophage polarization in tumour progression. *Semin Cancer Biol* 18, 349-355.

Tomlinson, M.L., Guan, P., Morris, R.J., Fidock, M.D., Rejzek, M., Garcia-Morales, C., Field, R.A., Wheeler, G.N., 2009. A chemical genomic approach identifies matrix metalloproteinases

as playing an essential and specific role in *Xenopus* melanophore migration. *Chem Biol* 16, 93-104.

Tonnesen, M.G., Feng, X., Clark, R.A., 2000. Angiogenesis in wound healing. *The journal of investigative dermatology. Symposium proceedings / the Society for Investigative Dermatology, Inc. [and] European Society for Dermatological Research* 5, 40-46.

Uong, A., Zon, L.I., 2010. Melanocytes in development and cancer. *Journal of cellular physiology* 222, 38-41.

Weis, S.M., Cheresh, D.A., 2011. Tumor angiogenesis: molecular pathways and therapeutic targets. *Nature medicine* 17, 1359-1370.

Yang, M., Baranov, E., Li, X.M., Wang, J.W., Jiang, P., Li, L., Moossa, A.R., Penman, S., Hoffman, R.M., 2001. Whole-body and intravital optical imaging of angiogenesis in orthotopically implanted tumors. *Proc Natl Acad Sci U S A* 98, 2616-2621.

Zhang, G., Miyake, M., Lawton, A., Goodison, S., Rosser, C.J., 2014. Matrix metalloproteinase-10 promotes tumor progression through regulation of angiogenic and apoptotic pathways in cervical tumors. *BMC cancer* 14, 310.

### **Figure Legends:**

**Figure 1: *In vivo* growth of 15/0 semi-solid tumor grafts. (A)** Representative images of collagen alone (I) and 15/0 tumor grafts (dashed white line) at day 3, 10, 16, 24 and 30 following engraftment (II-VI). Note the accumulation of melanophores in the tumor grafts at later time points. **(B)** Average increase in area  $\pm$ SEM of tumor or collagen only grafts determined over time relative to collagen only graft at day 0. Values are expressed as the mean  $\pm$  SEM from 15 animals in 3 independent experiments. P values calculated using students TTEST. LG-15, stage 54 (2 week old) tadpoles were subcutaneously grafted with 500,000 cells of 15/0 tumor while control animals were grafted with equal volume of collagen alone. Animals were imaged on a Nikon SMZ1500 stereomicroscope.

**Figure 2: Characterization of 15/0 tumor cells within the semi-solid tumor graft. (A)** Semi-solid tumors containing 500,000 15/0 tumor cells were either grown for 9 days *in vitro* (I and IV) or grafted subcutaneously *in vivo* in LG-15 tadpoles (II and V). Control collagen mass without tumor cells was maintained *in vitro* (III and VI). Semi-solid tumors were then stained with 0.1 $\mu$ g/ml DAPI (II, IV, and VI) and cells visualized using a Leica DMIRB inverted fluorescence microscope. **(B)** H&E staining of cryosections of tumor collagen grafts 3, 10, 16 and 30 days post transplantation (I-IV). Magnified images of boxed section from above panel (V-VIII). Slides were imaged using an Axiovert 200 inverted microscope. **(C)** Gömöri trichrome staining of cryosections of tumor collagen grafts 3, 10, 16 and 30 days post transplantation (I-IV). Magnified images of boxed section from above panel (V-VIII). Slides were visualized using an Axiovert 200 inverted microscope.

**Figure 3: Neo-angiogenesis in 15/0 collagen grafts.** LG-6 or LG-15 tadpoles were grafted with tumor grafts containing 500,000 15/0 tumor cells and animals were intracardiacally injected with either Texas red 70KDa or TMR 2000KDa dextran and imaged. **(A)** *Ex vivo* images of vascularized grafts from LG-15 tadpoles at day 7 post transplantation. PKH-labeled 15/0 cells (I) with Texas red-dextran filled vasculature (II). Vascularized tumors were imaged *ex vivo* using an Olympus BX40 conventional fluorescence microscope. **(B)** Intravital imaging of vasculature in LG-6 15/0 collagen grafted animals. Bright field image of vasculature entering tumor mass (I). Texas-red dextral filled vasculature entering semi-solid tumor (dashed line indicates tumor boundary) (II). Texas-red dextral filled vasculature within tumor mass (III). Black cells are melanophores within the tumor graft. Animals were imaged using a Nikon TE2000-U epifluorescence microscope. **(C)** TMR loaded vasculature within 15/0-collagen tumors in LG-6 tadpoles showing SHG signal (I), CFSE labeled tumor (II) and TMR loaded vessels (III) from 15/0-collagen tumor bearing animals. Animals were imaged using an Olympus two-photon laser-scanning microscope. Images from representative animals shown.

**Figure 4: Accumulation of melanophores in growing 15/0 tumor graft.** **(A)** 15/0 tumor graft heavily infiltrated by host melanophores at 30 days post-transplantation. **(B)** *Ex vivo* bright field imaging of a tumor graft showing melanophore (black arrow) accumulation within the 15/0 WT tumor (\*; delimited by a dashed white line) compared to normal skin melanophores (blue arrow). **(C)** One week *in vitro* culture of tadpole melanophores (m) derived from a semi-solid 15/0 tumor grafted into a LG-15 tadpole recipient that was invaded by melanophores as shown in A. Not the presence of numerous of other cells including 15/0 tumor cells (black arrows) and tumor infiltrating leukocytes (red arrows) **(D)** Melanophore (m) enriched three weeks *in vitro* culture of

15/0 tumor graft-derived melanophores. Note that only a few fibroblast (f) besides melanophores. Animals were imaged using the Nikon SMZ1500 stereomicroscope and cells with an Olympus BX40 microscope.

**Figure S1: Immobilization of tumor cells on a collagen matrix.** A collagen solution was made by adding setting solution Type I rat tail collagen in order to initiate the pH dependent polymerization. Tumor cells were then mixed with the collagen solution at a concentration of 500,000 cells per 10 $\mu$ L graft. Collagen/tumor mix was then pipetted into individual wells of 6 well plates and incubated at 27°C for 30 min to allow collagen polymerization. Two milliliters of media, was added to tumor collagen grafts. Plates containing the grafts were then incubated at 27°C in chambers containing a blood gas mix (5% CO<sub>2</sub>, 21% O<sub>2</sub>, 74% N) until use. Small subcutaneous incisions were made on anterior left or right region of tadpoles and the collagen tumor grafts were inserted subcutaneously within the incisions.

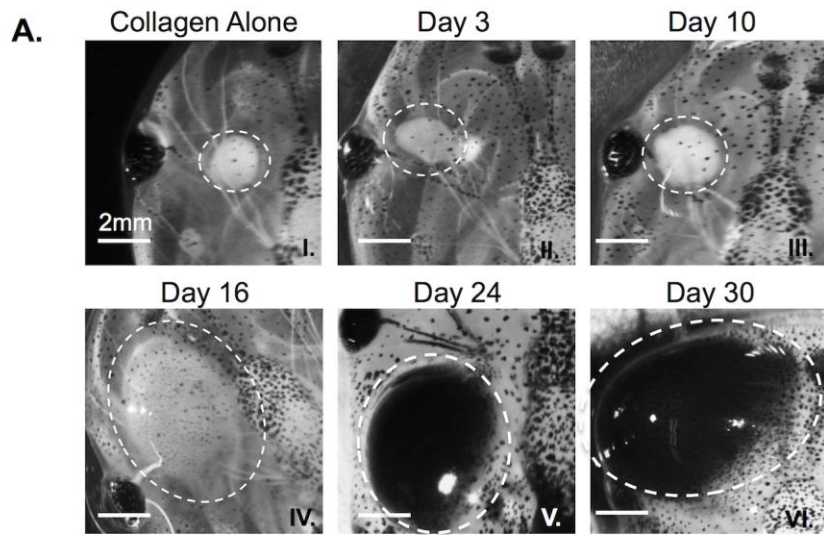
**Figure S2: Intra vital imaging of semi-solid 15/0 tumor cells in LG-6 tadpoles.** Semi-solid grafts containing 15/0 tumor cells labeled with 40 $\mu$ M CFSE labeled were grafted into LG-6 tadpoles. Animals were intra vitally imaged one-week post transplantation using a two-photon microscope. SHG of collagen (I) and CFSE fluorescence (II) within LG-6 tadpoles. Arrow indicates melanocyte.

**Figure S3: *Ex vivo* neovasculature in 15/0 collagen grafts.** Images of vascularized grafts at day 5 (A) and day 7 (B-C) post-transplantation. PKH-labeled 15/0 cells (I, IV and VII) with Texas red-dextran filled vasculature (II, V and VII). Collagen grafts containing PHK-labeled 15/0 Tumor cells were subcutaneously implanted into LG-15 tadpoles. At varying times post-engraftment animals were intracardiacally injected with Texas red 70KDa dextran. Ten minutes post injection, grafts were surgically removed, mounted on slides and imaged for fluorescence. Vascularized tumors were imaged *ex vivo* using an Olympus BX40 conventional fluorescence microscope.

**Figure S4: Representative intra vital images of normal vasculature and non-tumor embedded collagen.** (A) Texas red dextran loaded vasculature within tadpoles. (B) SHG from collagen only grafted animal.



Figure 1



**B.**

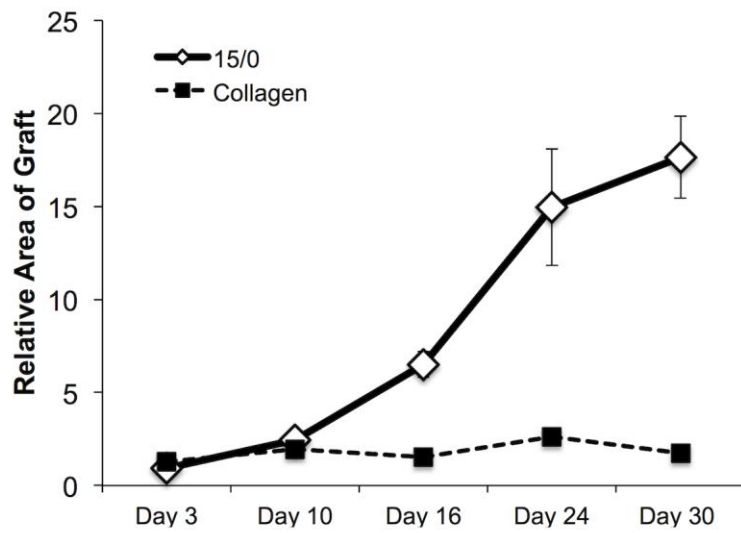


Figure 2

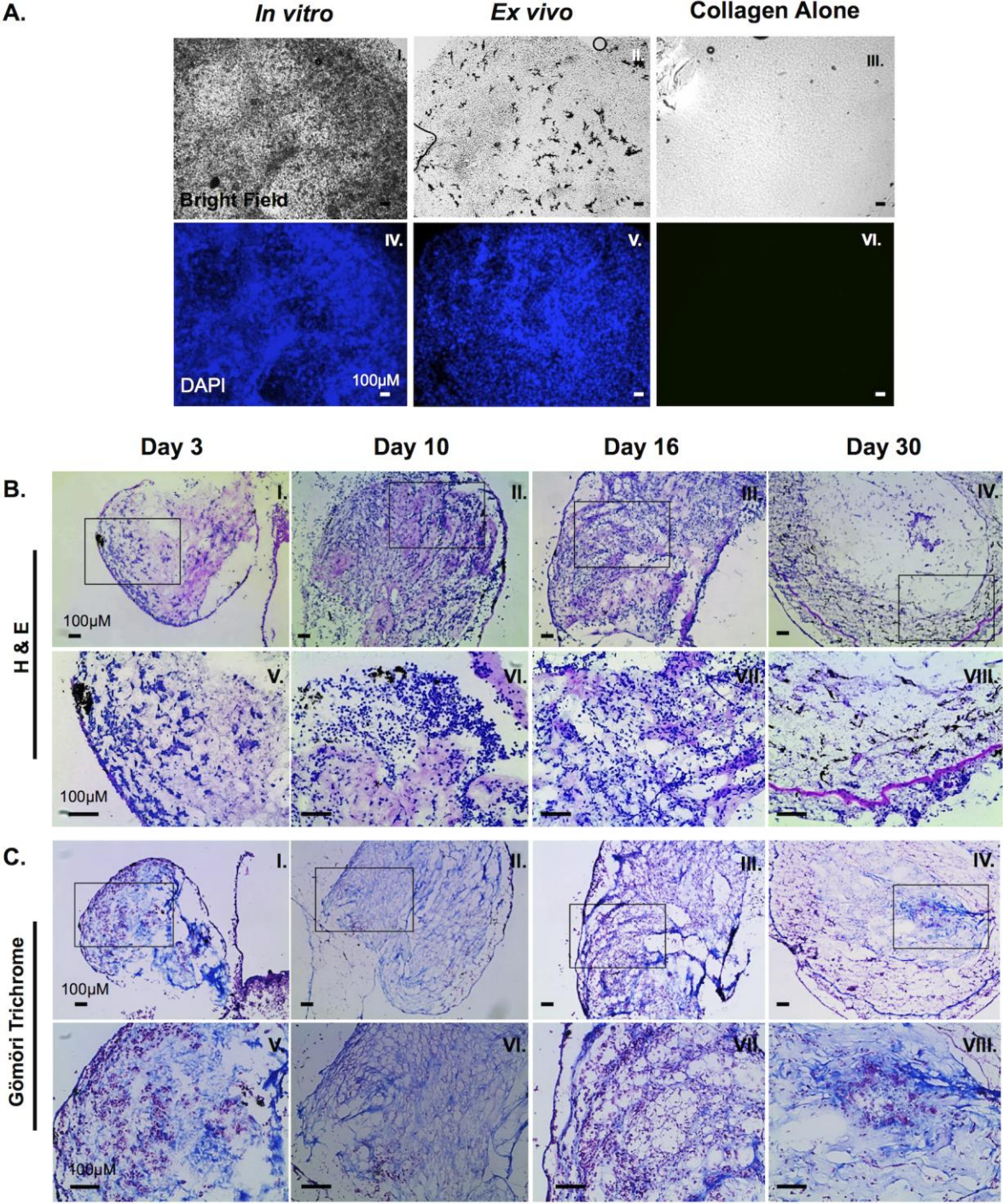


Figure 3

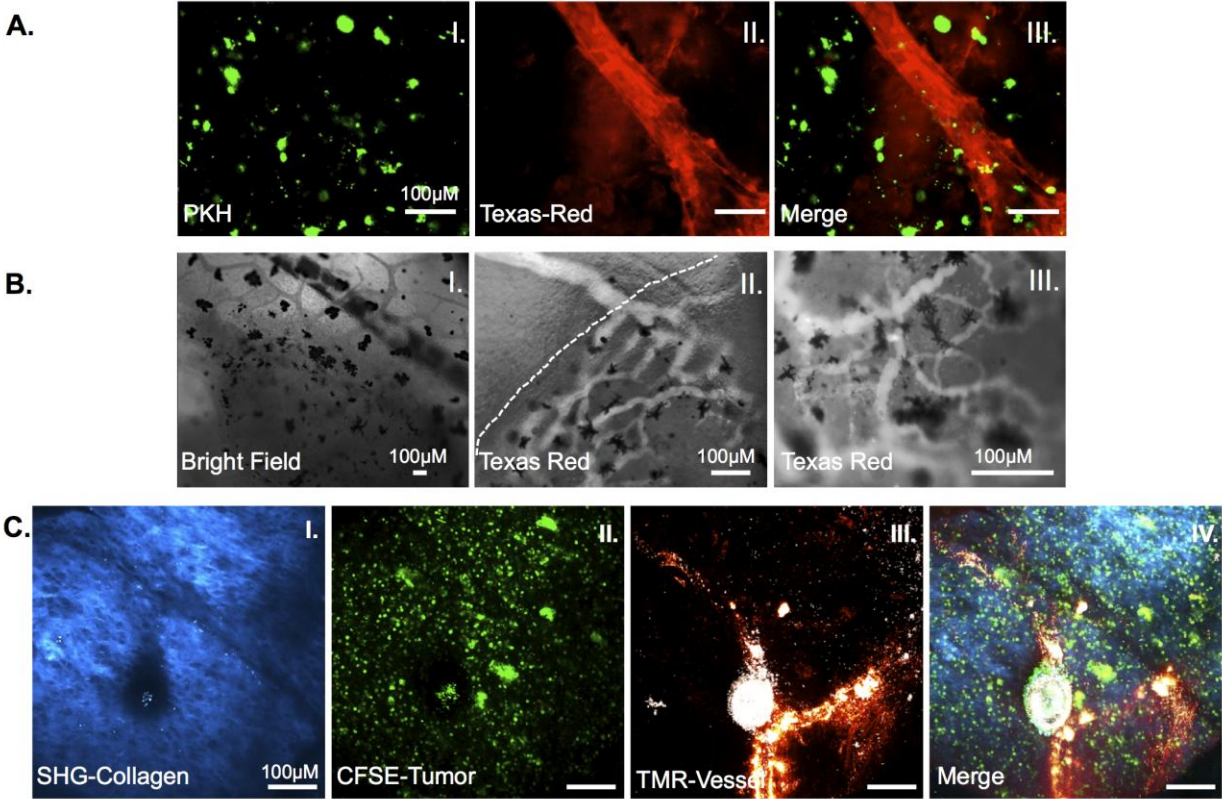
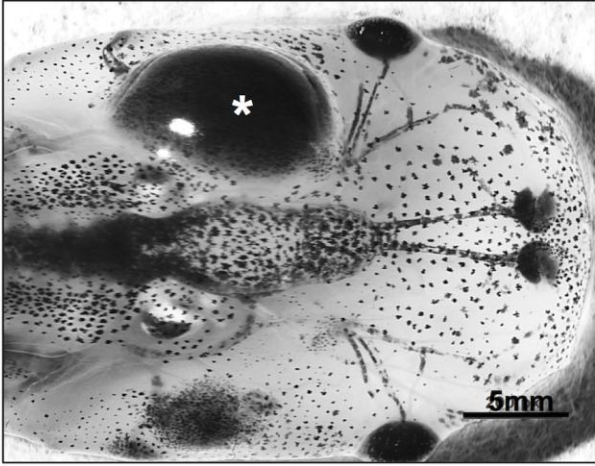


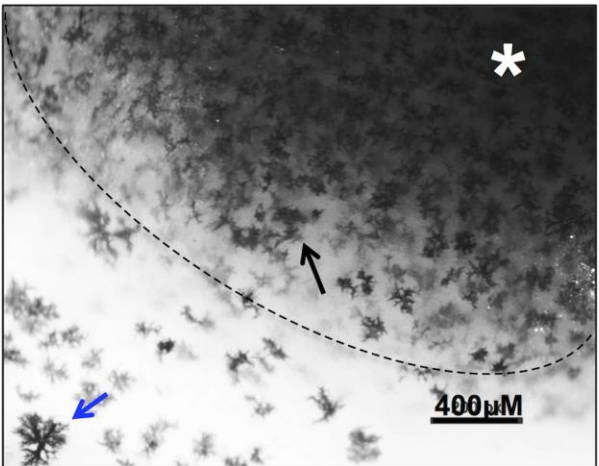


Figure 4

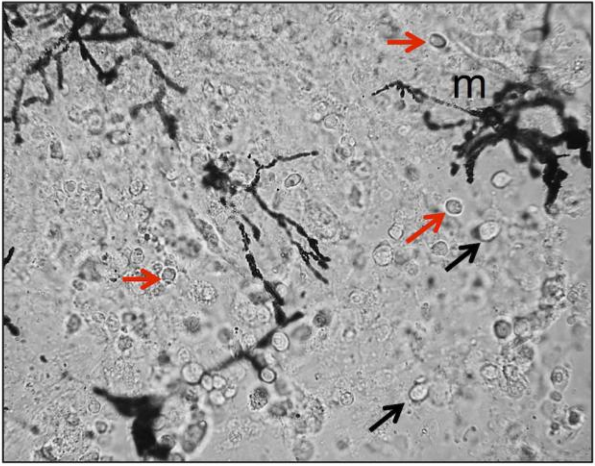
A.



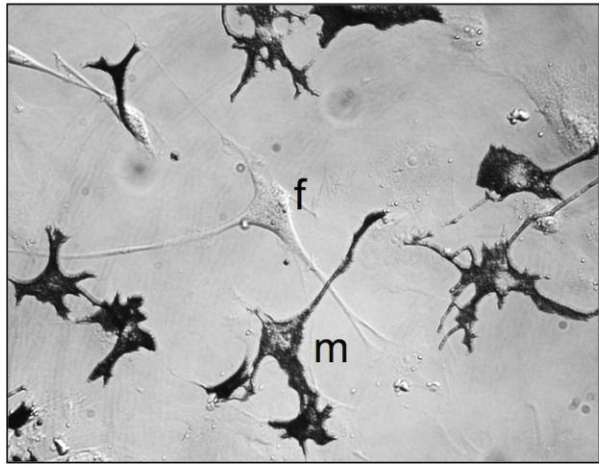
B.



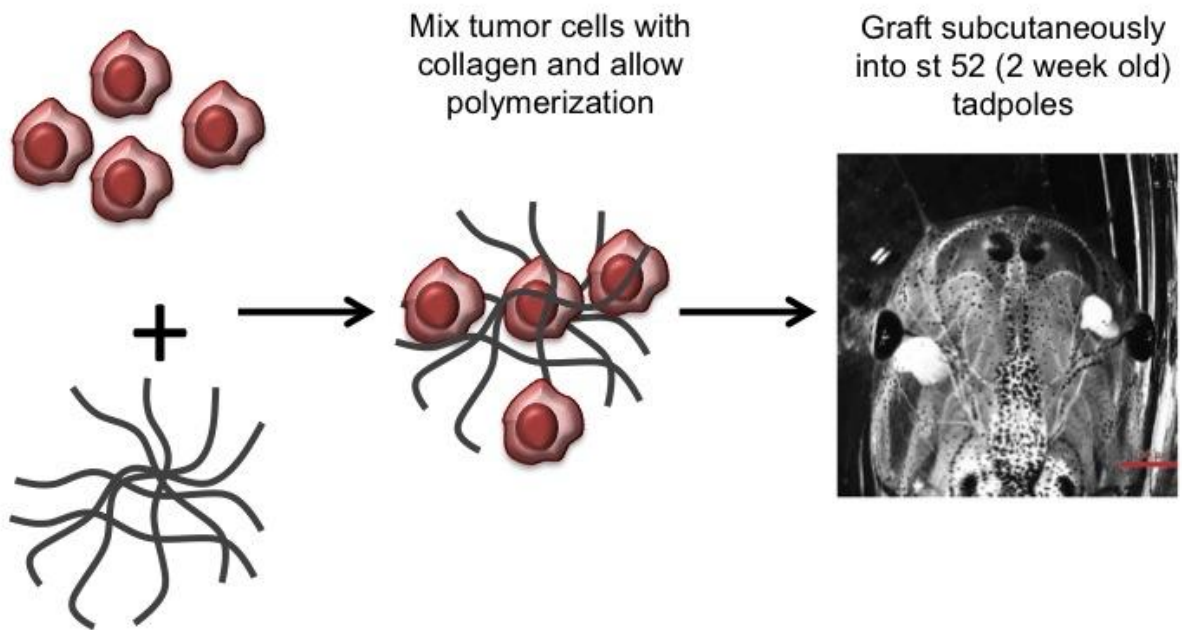
C.



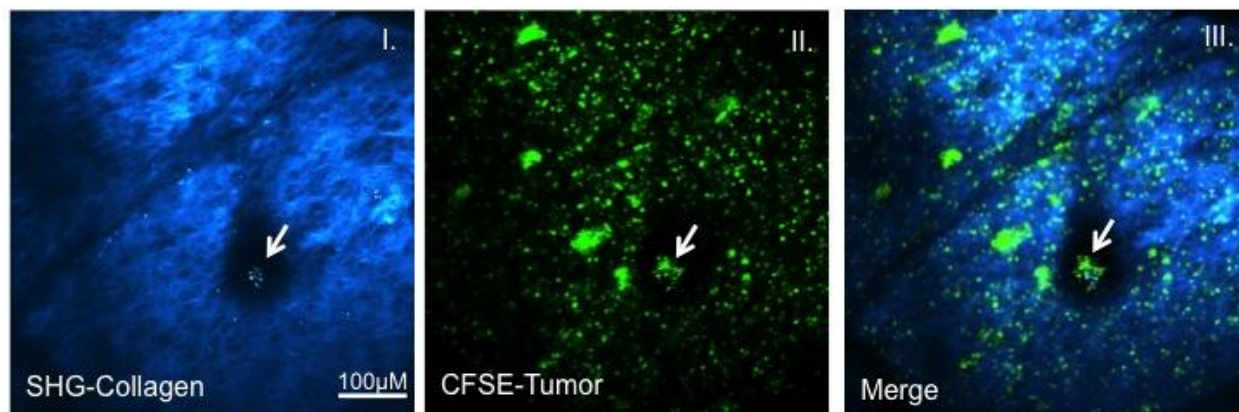
D.



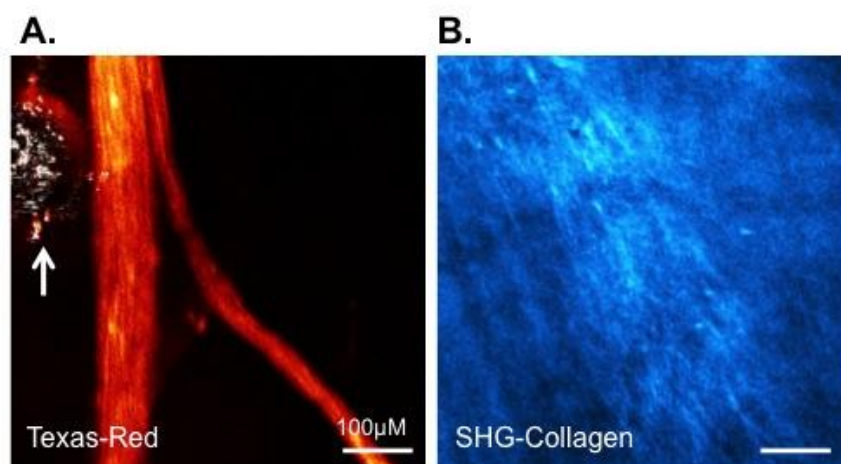
Supplementary Figure 1



## Supplementary Figure 2



Supplementary Figure 3



Supplementary Figure 4

